A&A 445, 819–825 (2006)
DOI: 10.1051/0004-6361:20053623

Astronomy & Astrophysics

Identification and study of systems of galaxies in the Shapley supercluster⋆

C. J. Ragone[1,2], H. Muriel[1,2], D. Proust[3], A. Reisenegger[4], and H. Quintana[4]

[1] Grupo de Investigaciones en Astronomía Teórica y Experimental, IATE, Observatorio Astronómico, Laprida 854, Córdoba, Argentina
[2] Consejo de Investigaciones Científicas y Técnicas de la República Argentina
e-mail: [cin;hernan]@oac.uncor.edu
[3] GEPI, Observatoire de Paris-Meudon, 92195 Meudon Cedex, France
e-mail: Dominique.Proust@obspm.fr
[4] Departamento de Astronomía y Astrofísica, Pontificia Universidad Católica de Chile, Casilla 306, Santiago 22, Chile
e-mail: [areisene;hquintana]@astro.puc.cl

Received 13 June 2005 / Accepted 7 September 2005

ABSTRACT

Based on the largest compilation of galaxies with redshift in the region of the Shapley Supercluster (Proust et al. 2004, P2004), we identified 122 galaxy systems, 60 of which are new systems. Using the SuperCOSMOS catalogue, we have assigned b_j magnitudes to each galaxy in our compilation. The sample of galaxy systems was used to estimate the mass function of systems in the range 10^{13} to 10^{15} $M_\odot\,h^{-1}$. We computed a lower value to the total mass in the region of the Shapley Supercluster with this mass function. Using 15 mock catalogues we derived the mean mass that these kinds of systems have before comparing it with that obtained from the real data.

Key words. galaxies: clusters: general

1. Introduction

The Shapley Supercluster (hereafter SSC) has the highest concentration of clusters and groups of galaxies in the local universe. It is centrally dominated by three Abell clusters (A3556, A3558, and A3562) and contains more than 20 Abell clusters. This supercluster has an extent of ∼20 Mpc, or even larger, and has not yet virialized. Kull & Böhringer (1999) analyzed a region of 6×3 degrees and found evidence of X-ray emission connecting the three central clusters of the SSC, indicating that the inter-cluster gas is being warmed up. Therefore, the core of the supercluster is in the procces of virialization.

A mass estimate of the SSC is particularly interesting due to its proximity to the local group. Moreover, it can be used to constrain theoretical models that should be able to predict this type of mass concentrations. Nevertheless, the fact that superclusters are not virialized systems seriously limitats the possible methods that can be used to estimate the mass. Bardelli et al. (2000) used galaxy counts to suggest that the SSC has a significantly higher mean density than the cosmic average. Reisenegger et al. (2000) (R2000 hereafter) applied the spherical collapse model and found that the mass enclosed by a radius of 8 h^{-1} Mpc is in the range 2.0×10^{15} to 1.3×10^{16} $M_\odot\,h^{-1}$, representing an overdensity range $\rho/\rho_c \sim 3$–20. In this work we explore an alternative way to estimate a lower limit to the total mass of the SSC. In a high mass concentration like the SSC, a significant fraction of galaxies are supposed to belong to groups or clusters of galaxies and, therefore, the mass function of these systems can be used to provide a lower limit to the total mass of the supercluster. In order to select a sample of galaxy systems that is as complete as possible, we used the resent catalogue by Proust et al. (2004, hereafter P2004). These authors compiled the largest velocity catalogue in the region of the SSC. It contains radial velocities for 8341 galaxies and represents a powerful tool for identifying and studying the galaxy systems in the SSC.

Large redshift surveys like 2dFGRS (2 degree Field Galaxy Redshift Survey) and SDSS (Sloan Digital Sky Survey) have stimulated the identification of galaxy groups based on the friends-of-friends algorithm (FOFA). The original algorithm introduced by Huchra & Geller (1982) was modified by Merchán & Zandivarez (2002) to take the sky coverage of 2dFGRS into account. Using mock catalogues, this technique has been extensively tested and has demonstrated its robustness in identifying galaxy groups in redshift space (see for instance Nolthenius & White 1987).

The aim of this work was to identify and study galaxy systems in a 12×15 degrees region of the SSC, based on the

⋆ Tables 1 and 2 are only available in electronic form at http://www.edpsciences.org

redshift compilation of P2004. The resulting catalogue was used to estimate a lower boundary to the total mass of the SSC. The outline of this paper is as follows. A description of the SSC is given in Sect. 2. Details of the simulation and the mock catalogue construction are described in Sect. 3. A brief description of the identification process for both observational data and mock catalogues is presented in Sect. 4. In Sect. 5 we analyse and estimate the mass enclosed by the SSC, and finally in Sect. 6 we discuss our main conclusions.

2. Observational data

The compilation of P2004 contains 8341 galaxies with redshifts taken from Quintana et al. (1995, 1997, 2000), Proust et al. (2004), Drinkwater et al. (1999, 2004), Watson et al. (2000), Bardelli et al. (1998, 2000, 2001), Kaldare et al. (2003), and data from the NED NASA/IPAC database. The P2004 catalogue covers a region of 12×30 degrees on the sky, where half of the galaxies are members of the SSC, with velocities within 9000 and 18 000 km s^{-1} s^{-1}. The main region is centered at $v = 14\,500$ km s^{-1}.

After taking the numerous sources involved in the P2004 compilation into account, a non-uniform redshift completeness is expected. The P2004 compilation overlaps the SuperCOSMOS Sky Survey (hereafter SSS) completely. Therefore, in order to test the redshift incompleteness we have assigned the corresponding magnitude in the SSS survey to each galaxy in the P2004 catalogue. Since none of the sources of the P2004 compilation includes faint galaxies, the cross correlation with the SSS was performed selecting galaxies brighter than $b_j = 19$. Using a matching radius of 10 arcsec, we found a positive cross-correlation between P2004 and SSS for more than 96% of the galaxies. Of these objects, 14% correspond to multiple identifications. After visually inspecting several images of multiple identifications we introduce several criteria based on the matching radius and the magnitudes in order to correctly assign the SSS galaxy. We estimated that more than 95% of the Shapley galaxies have been correctly identified in the SSS.

With the aim of performing a completeness mask, we used the HEALPix tool to produce an equal-area pixelisation of the sky. For each pixel of 2.6×10^{-4} strd, we counted galaxies up to a designed apparent magnitude limit, defining the completeness in a pixel as the ratio of the number of galaxies in the SSC to the number of galaxies in the SSS survey. The resulting mean completeness for an apparent magnitude limit of 17.5 is ∼0.5. The fraction of galaxies with measured redshift significantly decreases for fainter magnitudes. It should be noted that the completeness is not uniform, so it shows a tendency to be higher in the high density regions of the SSS.

3. Mock catalogues

In this study we used one of the publicly available Very Large Simulations (VLS) (Yoshida et al. 2001). Briefly, this simulation models a box of 479 Mpc h^{-1} in size, with 512^3 particles, each of mass $6.86{\times}10^{10}\ M_\odot\, h^{-1}$. Given the success of the model at reproducing observational data, we chose the ΛCDM scenario with cosmological parameters: $\Omega_\mathrm{m} = 0.3$, $\Omega_\Lambda = 0.7$, normalization $\sigma_8 = 0.9$, and $H_0 = 70$ km s^{-1} Mpc^{-1}.

Due to the large box size, it was possible to find a large number of rich systems, so we chose those that represent high density regions. R2000, using estimates of the SSC mass enclosed by 8 Mpc h^{-1}, find a density range $\rho/\rho_\mathrm{c} \sim 3{-}20$. The lower limit of this range corresponds to the Diaferio and Geller method (1997), whilst the upper one is obtained using the spherical collapse model (for more details see R2000).

Following these authors, we searched in the simulation for overdense regions in spheres of a radius of 8 Mpc h^{-1} and selected 14 of them with overdensities in the mentioned range. We refer positions to a coordinate system situated 145 Mpc h^{-1} away from the sphere center in order to mimic the real position of the SSC, and we selected a cone-shaped volume which subtended 20 Mpc h^{-1} of radius at the distance of the sphere center. Within this volume, overdensities ranged from $\rho/\rho_\mathrm{c} \sim 0.5$ to 1.1. Finally, we assigned particles within this volume a luminosity function that can be described by a Schechter fit with parameters $\alpha = -1.19$ and $M^*_\mathrm{b} = -19.79$ (Madgwick et al. 2002). The adopted $k + e$ correction was taken from (Norberg et al. 2001) and is given by the equation

$$k(z) + e(z) = \frac{z + 6z^2}{1 + 20z^3}. \tag{1}$$

A set of 15 mock catalogues was constructed from this data. Galaxies were selected within the described volume by applying the apparent magnitude limit of the SSC survey. The redshift incompleteness of the SSC was not reproduced in the mock catalogues due to the non-uniformity of the sample (i.e. high density regions show a higher completeness on average). In the following analysis, we select galaxies brighter than $m_\mathrm{b} = 17.5$ in both mocks and real data. The mean redshift completeness for the SSC subsample is ∼0.5.

4. Identification of galaxy groups

The completeness mask described in Sect. 2 allows us to identify galaxy groups in the SSC following the procedure described in Merchán & Zandivarez (2002). According to these authors, the identification can be performed using a similar algorithm similar to the one developed by Huchra & Geller (1982) but modified in order to take the incompleteness of the galaxy sample into account by introducing a correction in the linking lengths' scale factor. The algorithm links pairs of galaxies according to the following conditions:

$$D_{12} = 2 \sin\left(\frac{\theta_{12}}{2}\right) \frac{V}{H_0} \leq D_L = D_0 R \tag{2}$$

$$V_{12} = |V_1 - V_2| \leq V_L = V_0 R \tag{3}$$

where θ_{12} and V are the angular separation and the mean radial velocity, respectively; D_0 and V_0 are the transversal and radial linking cut-off at the fiducial velocity V_f. Scale factor R is introduced to compensate for the decline in the selection

function with distance. In this case the scaling factor is computed as

$$R = \left[\frac{\int_{\infty}^{M_{12}} \phi(M)\mathrm{d}M}{\int_{\infty}^{M_{\rm lim}} \phi(M)\mathrm{d}M} \frac{(C_1 + C_2)}{2} \right]^{-\frac{1}{3}} \quad (4)$$

where $M_{\rm lim}$ and M_{12} are the absolute magnitude of the brightest galaxy visible at distances $V_{\rm f}/H_0$ and V/H_0, respectively. The $(C_1 + C_2)/2$ factor in the previous equation corresponds to the correction introduced to the original Huchra & Geller (1982) algorithm to take the incompleteness of the sample into account, C_1 and C_2 are the completeness values in the direction of each galaxy. Finally D_0 and V_0 are the corresponding linking lengths at the fiducial velocity $V_{\rm f}$ and $\phi(M)$ is the luminosity function of the sample.

In this particular case, given the irregularity of the sky coverage, the remarkably rich concentration of galaxies and the large mass system range in the SSC, we need to take special care override misidentifications and spurious merging. In order to optimize the identification of systems, we took into account the X-ray flux contour plot of the Shapley Supercluster core by Kull & Böhringer (1999). We performed a series of system identifications in this same region using different linking length values V_0 and D_0, where D_0 is related to the number density contour surrounding a group relative to the mean number density ($\delta\rho/\rho$).

We found that standard values of $\delta\rho/\rho$ (∼80) caused the two central groups (SC1329-313 and SC1327-312) in the Kull & Böhringer (1999) plot to merge into a single system. In order to find a fair number of groups and to ensure that most of them are single dynamical systems, we selected the lowest overdensity that does not merge those X-ray systems that appear as single systems. Despite this, this choice yields a high value of $\delta\rho/\rho \sim 400$, which ensures small groups will be identified in a correctly.

Figure 1 shows the best correlation between the identified systems and the X-ray contours of Kull & Böhringer (1999). Identification of these systems corresponds to a transversal and a line-of-sight linking lengths of $D_0 = 0.14$ Mpc h^{-1} and $V_0 = 200$ km s^{-1}, respectively.

As a result of the identification process we found 122 systems of galaxies containing at least 4 members. The number of systems drops to 73 when considering groups within the $9000 < vr < 18\,000$ range. The spatial distribution of these groups is illustrated in Fig. 2, whereas Fig. 3 shows the distribution normalized to the total number of groups of their main properties: radial velocity, velocity dispersion, virial radius, and virial mass. In the same figure we plot (dotted line) the distributions corresponding to groups identified in the mock catalogues, again normalized to the total number of groups in the mocks. We can see a lack of low-mass systems in the SSC distributions, which is likely to be produced by the bias in the completeness of the sample. In Fig. 4, groups (dots) are overlapped with the completeness mask, Where we can appreciate a tendency of groups to correlate with the regions of higher completeness. This effect is the result of at least two processes: i) the FOFA algorithm tends to be more efficient in the regions of higher completeness and; ii) the compilation of P2004 has higher completeness in high density regions, where most of the galaxy systems are present.

The following are median values of the properties listed before for both mock and real samples, median dynamical properties of SSC groups are higher given the lack of small systems mentioned above:

$Vr_{\rm SSC} = 14\,597.8$ km s^{-1} $\quad Vr_{\rm mock} = 14\,370.9$ km s^{-1}
$\sigma_{\rm SSC} = 344.6$ km s^{-1} $\quad \sigma_{\rm mock} = 200.8$ km s^{-1}
$R_{\rm vir-SSC} = 0.78$ Mpc h^{-1} $\quad R_{\rm vir-mock} = 0.57$ Mpc h^{-1}
$M_{\rm vir-SSC} = 4.6{\times}10^{13}\, M_\odot\, h^{-1}$ $\quad M_{\rm vir-mock} = 1.4{\times}10^{13}\, M_\odot\, h^{-1}$.

Table 1 shows the different properties of the galaxy systems identified in the SSC sample. As noted before, if we restrict the sample to the Shapley Supercluster region ($9000 < v_{\rm r} < 18\,000$), the resulting number of systems is 73. We performed a cross correlation between our catalogue and the NED NASA/IPAC database, using a search radius of 20 arcsec and a $\Delta v_{\rm r} \leq 2000$ km s^{-1}. The last restriction was only applied to those systems in the NED with known redshift. We found that 60 of the 122 are new galaxy systems. Of the 62 already known systems, 37 were identified as clusters, althoug, many of them were also identified as group. (34 are Abell clusters). The remaining 25 were only identified as groups. Table 2 shows the name of the systems (Col. 2), the type of system, the mean radial velocity, and the difference in the central position (Cols. 3−5, respectively).

5. Mass statistics

In this section we compute the mass function of groups in the SSC and use it to estimate a lower limit to the total mass of this system. We used the mock catalogues and the simulation described in Sect. 3 in order to compute the real mass enclosed in a volume like the SSC one and to compare with the inferred mass. The group mass function was derived using the $1/V$max method, which has the advantage of being a non-parametric procedure, i.e. it does not assume a shape of the mass function. Moreover, it not only gives shape but also normalization at the same time. The differential mass function can be computed using the equation

$$\frac{\mathrm{d}N}{\mathrm{d}\mathcal{M}}(\mathcal{M}) = \sum_{|\mathcal{M}_i - \mathcal{M}| \leq d\mathcal{M}/2} \frac{1}{V_{\rm max}(M_i)} \quad (5)$$

where $\mathcal{M}_i$ and M_i are the group mass and absolute magnitude respectively, and

$$V_{\rm max}(M_i) = \int_{\min(z_2, z_{\rm max})}^{\max(z_1, z_{\rm min})} \frac{\mathrm{d}V}{\mathrm{d}z} \mathrm{d}z \quad (6)$$

is the maximum comoving volume, within the catalogue velocity cut-off, out to which the group i with magnitude M_i remains observed. Both z_1 and z_2 are the geometric limits of the sample, and $z_{\rm min}$ and $z_{\rm max}$ are found by solving the equations

$$M_i = \begin{cases} m_2 - 5\log d_L(z_{\rm max}) - 25 - k(z_{\rm max}) \\ m_1 - 5\log d_L(z_{\rm min}) - 25 - k(z_{\rm min}) \end{cases} \quad (7)$$

hence, $z_{\rm min}$ and $z_{\rm max}$ are the redshift of groups whose absolute magnitudes are identical to the one of the object being considered, but its apparent magnitudes are the bright (m_1) and faint (m_2) limits of the survey.

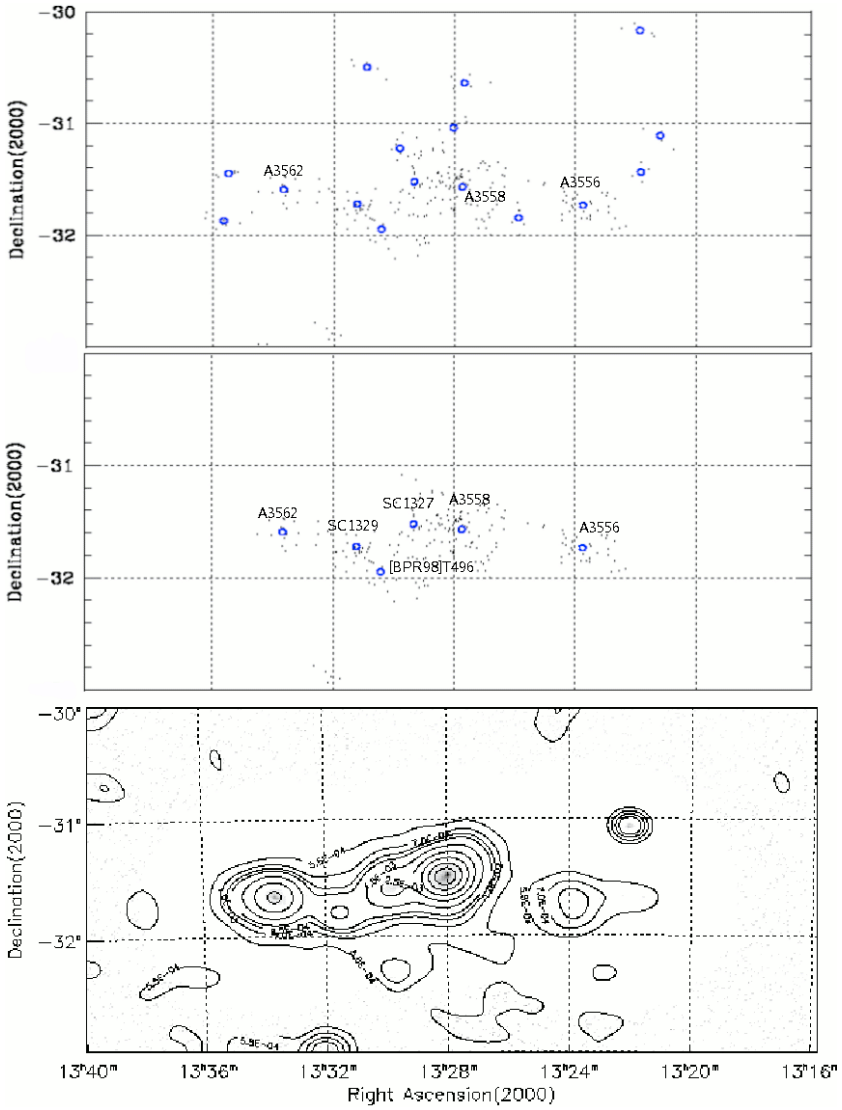

Fig. 1. *Lower panel*: X-ray contours of Kull & Böhringer (1999), for the central region of the SSC. *Middle panel*: SSC groups with at least 10 galaxies in the same region. *Top panel*: the same as the middle panel but considering groups with at least four members. Dots represent members of galaxy group and open circles the group centers.

Before using the $1/V_{\max}$ method, there are three intermediate issues to resolve: namely, to calculate groups "apparent magnitudes", which can be inferred from groups luminosities, to find out the corresponding completeness limit of the sample, and to determine the geometric limits where the mass function is to be calculated. Regarding the former, we calculated the total luminosity $L_{\rm tot}$ for each group using the prescription outlined in Moore et al. (1993), as the sum of the luminosities of its galaxy members ($L_{\rm obs}$) plus the integrated luminosity of galaxies below the magnitude limit of the sample ($L_{\rm cor}$):

$$L_{\rm tot} = L_{\rm obs} + L_{\rm cor}. \tag{8}$$

$L_{\rm corr}$ is calculated assuming that group members are independently drawn from a Schechter fit to the luminosity function of galaxies in groups. Hence, for faint group members which can not be observed

$$L_{\rm cor} = N_{\rm obs} \frac{\int_0^{L_{\rm lim}} L\Phi(L)\mathrm{d}L}{\int_{L_{\rm lim}}^{\infty} \Phi(L)\mathrm{d}L} \tag{9}$$

where $L_{\rm lim} = 10^{0.4(M_\odot - M_{\rm lim})}$, $M_{\rm lim} = m_{\rm lim} - 25 - 5\log[d_L(z)]$, and $M_\odot$ is the absolute magnitude of the sun in the corresponding band. Once the total luminosity of a group is obtained, we were able to compute its absolute magnitude, and finally, the group "apparent magnitude" using the distance modulus. As it relates to the "apparent magnitude" limit of the group sample, we used the completeness test developed by Rauzy (2001), which can be applied to any redshift-space distribution and used for any selection function. It is assumed that the luminosity function of the population depends neither on time nor on the spatial position of the objects; peculiar velocities of the observed redshifts are negligible, and the sample is complete in apparent magnitude up to a given magnitude limit $m_{\rm lim}$.

The principle of the method consists of defining the random variable

$$\zeta = \frac{F(M)}{F[M_{\rm lim}(Z)]} \tag{10}$$

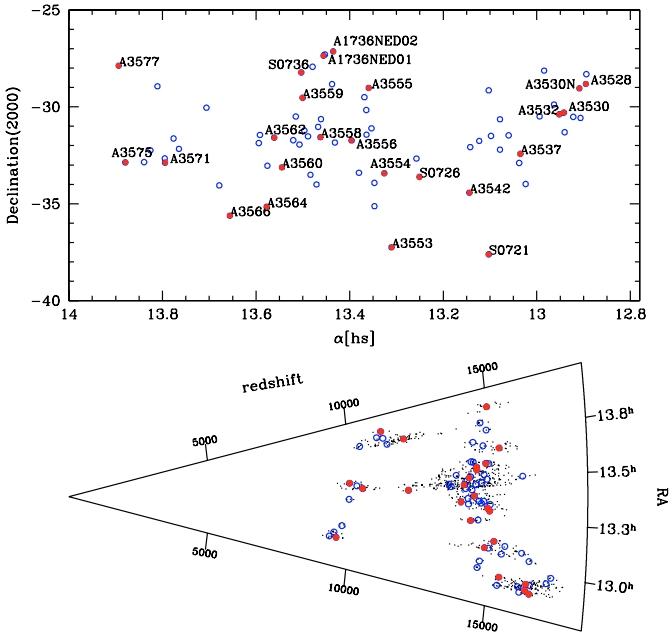

Fig. 2. The spatial distribution of groups with at least 4 members and within a velocity range $9000 < V_r < 18\,000$. Open circles represent group centers and filled circles the known ACO clusters; in the lower panel dots correspond to members of galaxy group.

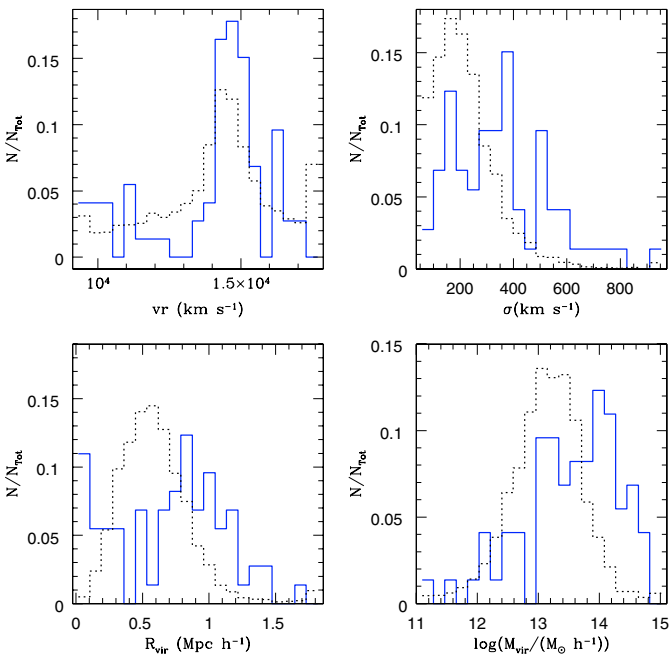

Fig. 3. Histograms showing the distributions of groups redshifts (*upper left panel*), velocity dispersions (*upper right panel*), virial radii (*lower left panel*), and virial masses (*lower right panel*). Only groups with at least 4 members and within the velocity range $9000 < V_r < 18\,000$ were included. In all cases solid and dashed lines correspond to SSC and mock groups, respectively.

where $F(M)$ stands for the cumulative luminosity function, and $M_{\rm lim}(Z) = m_{\rm lim} - Z$, where Z is the distance modulus. The

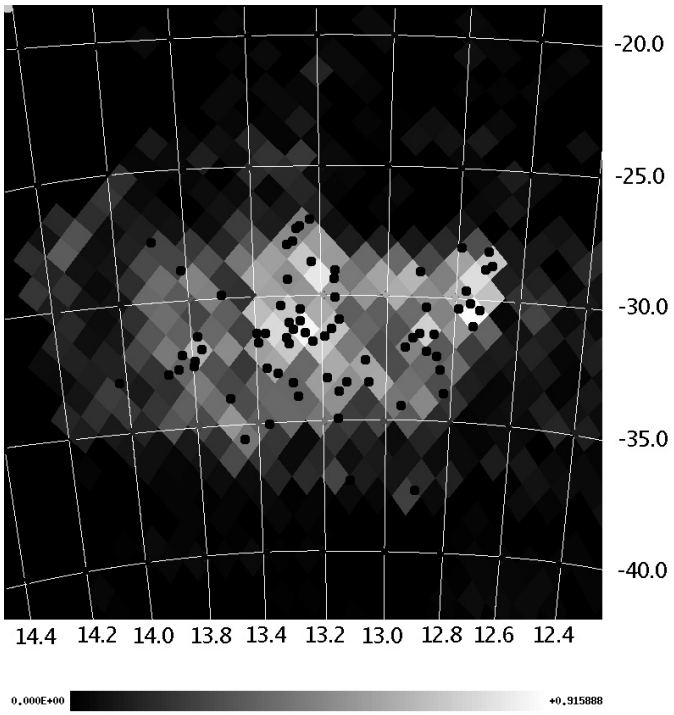

Fig. 4. Identified groups containing at least 4 members within the velocity range $9000 < V_r < 18\,000$, overlapped with the completeness mask derived in Sect. 2. Both α and δ units are hours and degrees, respectively. The bottom gray scale bar corresponds to the completeness level.

variable ζ can be estimated without any prior knowledge of $F(M)$, considering for each object the quantity

$$\hat{\zeta} = \frac{r_i}{n_i + 1} \tag{11}$$

where r_i is the number of objects satisfying $M \leq M_i$ and $Z \leq Z_i$, and n_i is the number of objects such that $M \leq M^i_{\rm lim}(Z_i)$ and $Z \leq Z_i$. The expectation of $\hat{\zeta}$ is $E_i = 1/2$ and its variance $V_i = \frac{n_i - 1}{12(n_i+1)}$. Hence, the quantity

$$T_{\rm C} = \frac{\sum_{i=1}^{N_{\rm gal}} (\hat{\zeta}_i - \frac{1}{2})}{(\sum_{i=1}^{N_{\rm gal}} V_i)^{\frac{1}{2}}} \tag{12}$$

has an expectation of zero and variance unity. The test requires the computation of $T_{\rm C}$ for subsamples that are truncated up to increasing values of the limiting apparent magnitude m_*. The $T_{\rm C}$ statistic is expected to be distributed around zero with dispersion of unity, as long as m_* remains below the completeness limit $m_{\rm lim}$. If m_* becomes greater than $m_{\rm lim}$, there will be a lack of objects with M fainter than $M_{\rm lim}$, resulting in a systematic decline of $T_{\rm C}$ towards negative values.

Figure 5 shows the result of aplying the $T_{\rm C}$ statistics to the SSC (solid line) and mock groups (dashed line). A systematic decline of the $T_{\rm C}$ statistics can be observed beyond $m = 14.3$ for SSC (vertical solid line). For groups in the M1 sample, the apparent magnitude cut-off is $m = 14.5$ (vertical dashed line). Horizontal lines are the 1σ limits of the $T_{\rm C}$ variance.

Finally, regarding the geometric limits of our flux-limited sample, we adopted the velocity range defined by

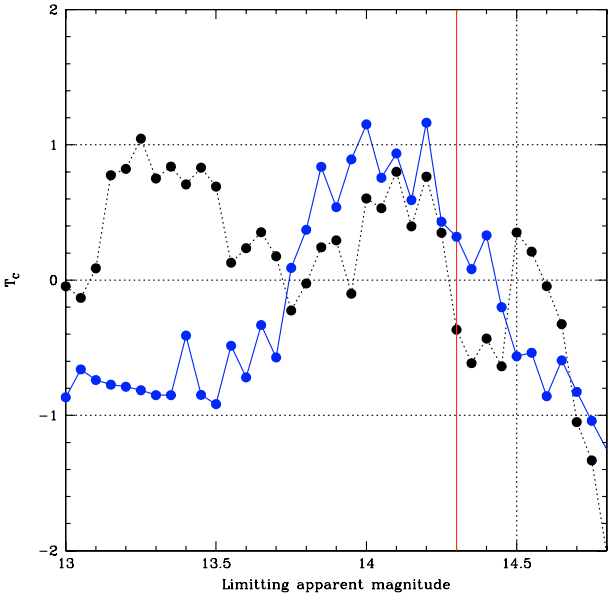

Fig. 5. Completeness test of Rauzy (2001). Solid and dotted lines correspond to SSC and mock groups, respectively. The vertical solid line denotes the adopted apparent magnitude limit for SSC, whereas the dotted vertical line is associated to mock groups. Horizontal lines are the 1σ limits of the T_C variance.

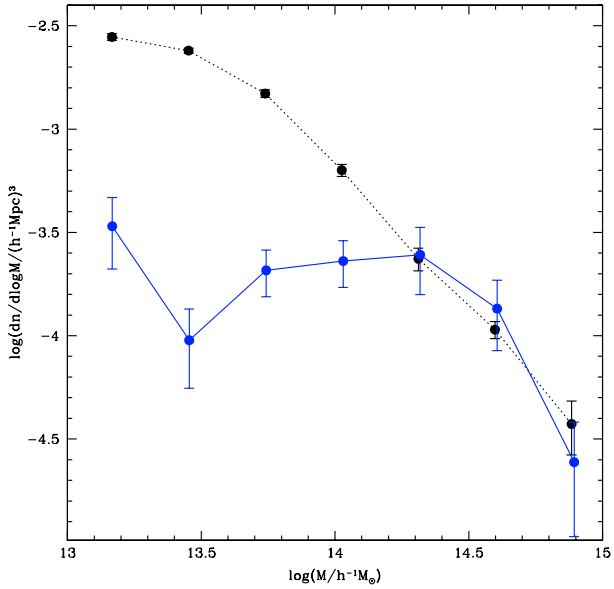

Fig. 6. The mass function for SSC (solid line) and mock groups (dotted line). Error bars were estimated by the bootstrap resampling technique.

Quintana et al. (2000), who consider as SSC members all galaxies in the redshift range $9000 < v < 18\,000$. Considering both, these redshift limits and the "apparent magnitude" cut-off, we computed the SSC mass function with 55 galaxy groups containing at least 4 members.

Results are shown in Fig. 6, where the SSC group mass function (solid line) is compared to the one obtained from the mock groups (dotted line, 2729 groups selected from a complete flux-limited sample of galaxies). We found that the obtained mass functions have different trends up to $M \sim 1 \times 10^{14}\ M_\odot h^{-1}$, while they are quite similar in the high mass region. The lack of groups in the low mass region of the SSC mass function was expected considering that the completeness is higher close to massive clusters and lower in the underdense areas of the SSC. Consequently, low mass groups are likely to be lost by the group finding process. Analysis of Fig. 6 leads us to conclude that the completeness mask is the primary responsible for the differences between the SSC and mock mass functions. Following this idea, and assuming that our mock catalogues correctly represent the SSC and then integrating the mock mass function in the considered volume, all should provide an estimate of the mass that is typical of systems like the SSC. The same procedure applied to the SSC group mass function yields a minimum mass, since as noted some of the SSC low mass groups are possibly missed given they have been poorly sampled. After performing these computations we obtained a mass of $\sim 1.1 \times 10^{16}\ M_\odot h^{-1}$ from the mock mass function, whereas the mass drops to a value of $4.8 \times 10^{15}\ M_\odot h^{-1}$ for the SSC; both of these masses consider systems with at least $1 \times 10^{13}\ M_\odot h^{-1}$.

Using the high density regions selected in the simulations, we find that ~60% of the particles in a 8 Mpc h^{-1} sphere are within groups of at least $1 \times 10^{13}\ M_\odot h^{-1}$, whereas this value drops to ~30% when considering the cone volume.

We can give a rough estimation of the total mass enclosed in the cone-volume we are using by considering the fraction of mass that, according to the simulation, we are missing. The final values that we find for our mock catalogues and the SSC are 3.7×10^{16} and 1.6×10^{16}, respectively.

R2000, using a spherical collapse model, state that the SSC mass enclosed by a radius of 8 Mpc h^{-1} lies between 2×10^{15} and $1.3 \times 10^{16}\ M_\odot h^{-1}$. Disregarding this for groups peculiar motions, we can roghly compute the mass within a sphere of radius 8 Mpc h^{-1}, centered as in R2000, by summing up the group virial masses. In so doing we obtain $2.3 \times 10^{15}\ M_\odot h^{-1}$, If we take into account the 40% of the mass that is not in galaxy systems, our derived value is 3.8×10^{15} for the SSC in a 8 Mpc h^{-1} sphere, a result in fair agreement with R2000.

6. Conclusions

Based on the compilation of redshift made by Proust et al. (2004), and assigning magnitudes from the SuperCOSMOS catalogue, we have identified galaxy systems in an area of 12×15 degrees. The transversal and line-of-sight linking lengths used to identified systems were $D_0 = 0.14$ Mpc h^{-1} and $V_0 = 200$ km s^{-1}, respectively. We identified 122 systems of galaxies with at least 4 members, and 73 of these are in the Shapley redshift range ($9000 < v_r < 18\,000$). 62 of the 122 are new systems. Of the remaining, 37 were previously identified as clusters (34 are Abell clusters). The velocity dispersion for the whole sample of galaxy systems spans a range from ~60 to 950 km s^{-1} with a median value of 344.6 km s^{-1}. The median virial radius and the median virial mass are 0.78 Mpc h^{-1} and $4.6 \times 10^{13}\ M_\odot h^{-1}$, respectively.

With the non-parametric $1/V_{max}$ method, we computed the mass function of galaxy systems in the SSC region, and we

found evidences of a possible bias in the number of low mass systems. This effect could be a consequence of the correlation between the redshift completeness and the galaxy density, present in the Proust et al. (2004) compilation. By integrating the derived mass function in the range 10^{13} to 10^{15} $M_\odot h^{-1}$, we found that the total mass of the SSC is on the order of 4.8×10^{15} $M_\odot h^{-1}$. Taking the possible bias in the identification of low mass systems into account and also that we are missing the mass outside galaxy systems, the last value should be taken as a lower boundary. Using the mock catalogues free of the redshift incompleteness, we found a mass of $\sim 1.1 \times 10^{16}$ $M_\odot h^{-1}$ in the same mass range as before. We estimated the fraction of galaxies/mass that, according to the numerical simulation, is outside galaxy systems. With this fraction to correct the SSC mass, we found a total mass of $\sim 1.6 \times 10^{16}$ $M_\odot h^{-1}$. In order to compare with the mass computed in R2000 using a spherical collapse model, we disregarded group peculiar motions and summed up the group virial masses. After correcting for the mass outside systems, we obtained 3.8×10^{15} $M_\odot h^{-1}$ for the SSC in the central 8 Mpc h^{-1} sphere, in agreement with their work.

Acknowledgements. The authors wish to thank the referee Dr. S. Bardelli for useful suggestions. The simulations used in this paper were carried out by the Virgo Supercomputing Consortium using computers at Computing Center of the Max-Planck Society in Garching and at the Edinburgh Parallel Computing Centre. The data are publicly available at www.mpa-garching.mpg.de/NumCos. This work was partially supported by the Agencia Nacional de Promoción Científica y Técnica, Secretaría de Ciencia y Técnica (SeCyT), Consejo de Investigaciones Científicas y Técnicas de la República Argentina (CONICET), Agencia Córdoba Ciencia, FONDAP Center for Astrophysics and FONDECYT grant # 1020840.

References

Bardelli, S., Zucca, E., Zamorani, G., Vettolani, G., & Scaramella, R. 1998, MNRAS, 296, 599
Bardelli, S., Zucca, E., Zamorani, G., Moscardini, L., & Scaramella, R. 2000, MNRAS, 312, 540
Bardelli, S., Zucca, E., & Baldi, A. 2001, MNRAS, 320, 387
Huchra, J. P., & Geller, M. J. 1982, ApJ, 257, 423
Diaferio, A., & Geller, M. J. 1997, ApJ, 481, 633
Drinkwater, M. J., Proust, D., Parker, Q. A., Slezak, E., & Quintana, H. 1999, PASA, 16, 113
Drinkwater, M. J., Parker, Q. A., Proust, D., Slezak, E., & Quintana, H. 2004, PASA, 21, 89
Kaldare, R., Colles, M., Raychaudhury, S., & Slezak, E. 1995, AJ, 110, 463
Kull, A., & Böhringer, H. 1999, A&A, 341, 23
Madgwick, D., Lahav, O., Baldry, I. K., et al. (the 2dFGRS Team) 2002, MNRAS, 333, 133
Merchán, M. E., & Zandivarez, A. 2002, MNRAS, 335, 216
Moore, B., Frenk, C. S., & White, S. D. M. 1993, MNRAS, 261, 827
Nolthenius, R., & White, S. 1987, MNRAS, 225, 505
Norberg, P., Baugh, C. M., Hawkins, E., et al. (the 2dFGRS Team) 2001, MNRAS, 328, 64
Proust, D., Quintana, H., & Reisenegger, A. 2004, in preparation
Quintana, H., Ramirez, A., Melnick, J., Raychaudhury, S., & Slezak, E. 1995, AJ, 110, 463
Quintana, H., Melnick, J., Proust, D., & Infante, L. 1997, A&AS, 125, 247
Quintana, H., Carrasco, E. R., & Reisenegger, A. 2000, AJ, 120, 511
Reisenegger, A., Quintana, H., Carrasco, E. R., & Maze, J. 2000, AJ, 120, 523
Rauzy, S. 2001, MNRAS, 324, 51
Watson, F. G., Parker, Q. A., et al. 2000, Proc SPIE, 4008, 123
Yoshida, N., Sheth, R., & Diaferio, A. 2001, MNRAS, 328, 669

Online Material

Table 1. Properties of SSGC groups.

SSGC number	RA (2000)	Dec (2000)	$\langle V_r \rangle$ [km s^{-1}]	σ_r [km s^{-1}]	Mass [$\times 10^{13}$ $M_\odot$]	#mem.	R_{vir} [Mpc]
1	185.799	–34.508	2799	179	3.19	10	1.42
2	187.332	–39.023	3277	170	3.19	14	1.56
3	191.622	–41.408	3322	732	76.24	30	2.03
4	190.763	–36.761	3293	97	0.18	4	0.28
5	192.786	–26.389	3169	85	0.39	5	0.78
6	193.412	–28.312	16 223	389	1.51	6	0.14
7	193.425	–28.817	16 566	169	0.03	4	0.01
8	193.635	–29.042	16 395	540	9.20	36	0.45
9	193.553	–29.841	21 147	338	0.19	5	0.02
10	193.598	–30.570	15 383	148	0.14	5	0.09
11	193.678	–28.985	22 582	366	15.94	4	1.70
12	194.133	–30.292	16 413	526	16.70	58	0.86
13	193.831	–30.514	16 122	98	0.01	4	0.01
14	194.106	–31.310	16 541	524	12.86	23	0.67
15	194.342	–32.792	22 808	332	10.06	8	1.30
16	194.280	–30.380	15 436	147	0.11	4	0.07
17	194.446	–29.878	17 133	336	8.07	7	1.02
18	194.360	–29.036	18 112	453	1.41	5	0.09
19	194.513	–28.502	20 241	437	2.65	14	0.19
20	194.529	–28.215	22 733	635	18.63	4	0.66
21	194.764	–28.129	14 677	57	0.12	4	0.54
22	195.290	–35.498	5064	371	9.64	4	0.99
23	195.118	–37.339	4369	491	19.10	4	1.13
24	194.909	–30.493	17 281	146	1.23	4	0.82
25	195.505	–32.259	4786	241	1.92	7	0.47
26	195.200	–31.361	3548	144	0.04	5	0.02
27	195.357	–33.981	14 704	126	1.59	4	1.42
28	196.075	–30.154	3391	300	2.69	26	0.42
29	195.525	–32.424	9567	280	0.41	4	0.07
30	195.408	–30.925	5193	132	0.06	6	0.05
31	195.581	–32.858	5024	189	0.30	6	0.12
32	195.563	–32.895	9323	211	1.10	4	0.35
33	195.901	–31.472	16 468	298	4.32	5	0.69
34	195.888	–34.011	24 113	226	0.77	7	0.21
35	196.179	–30.640	15 472	250	3.89	6	0.89
36	196.179	–32.209	9480	155	0.31	6	0.18
37	196.539	–37.610	14 912	726	39.37	22	1.06
38	196.465	–31.497	16 191	202	0.26	6	0.09
39	196.499	–34.264	25 883	173	0.29	5	0.13
40	197.069	–28.227	2217	87	0.04	7	0.08
41	196.541	–29.145	15 021	278	1.34	8	0.24
42	196.576	–29.571	20 468	500	13.11	6	0.75
43	196.844	–31.758	15 580	388	7.97	5	0.75
44	197.134	–32.077	9751	101	0.58	4	0.82
45	197.161	–34.430	15 192	270	2.56	5	0.50
46	197.799	–34.715	29 405	945	151.08	4	2.42
47	197.892	–34.343	27 159	724	57.04	4	1.55
48	199.394	–43.473	3508	438	13.25	8	0.98
49	198.483	–30.207	32 134	358	8.85	5	0.98
50	198.761	–33.616	14 331	263	4.64	4	0.96
51	198.858	–32.668	14 597	350	5.75	9	0.67
52	199.728	–25.120	1683	524	26.33	6	1.37
53	199.658	–37.252	15 055	523	17.72	9	0.92

Table 1. continued.

SSGC number	RA (2000)	Dec (2000)	$\langle V_r \rangle$ [km s^{-1}]	σ_r [km s^{-1}]	Mass [$\times 10^{13}$ $M_\odot$]	#mem.	R_{vir} [Mpc]
54	200.031	–27.576	1889	270	0.60	7	0.11
55	199.757	–34.566	7974	380	3.48	5	0.34
56	199.886	–33.428	14 928	323	5.82	9	0.80
57	200.205	–33.926	14 251	495	13.62	6	0.79
58	200.203	–35.123	15 033	229	4.34	4	1.17
59	200.299	–31.108	14 713	447	9.87	6	0.70
60	200.466	–30.165	14 627	305	4.67	4	0.71
61	200.387	–29.022	14 005	129	0.08	5	0.06
62	200.459	–31.435	14 798	382	9.49	4	0.93
63	200.529	–29.498	10 004	133	0.58	4	0.47
64	200.730	–34.911	8025	223	1.22	5	0.35
65	200.938	–31.731	14 454	491	16.59	37	0.98
66	200.699	–33.402	14 231	419	6.21	7	0.50
67	201.256	–30.196	4250	220	0.67	15	0.19
68	201.322	–33.725	7785	134	0.83	4	0.65
69	201.790	–27.299	13 690	787	47.09	43	1.08
70	201.472	–31.843	14 370	395	1.40	6	0.12
71	201.527	–27.136	12 160	225	2.52	4	0.71
72	201.563	–28.827	14 179	212	1.47	4	0.46
73	201.937	–31.567	14 094	910	67.17	91	1.16
74	201.837	–27.359	10 515	378	10.02	16	1.00
75	201.919	–30.635	14 514	377	1.33	6	0.13
76	201.891	–29.313	4156	338	3.27	4	0.40
77	202.187	–27.929	10 299	327	4.63	8	0.61
78	202.009	–31.035	13 560	512	15.70	5	0.85
79	202.063	–34.006	14 727	369	6.35	5	0.66
80	202.255	–33.507	14 197	344	5.86	4	0.70
81	202.335	–31.521	14 913	576	30.25	26	1.30
82	202.607	–31.946	14 325	763	47.19	25	1.16
83	202.807	–31.720	13 819	682	37.26	26	1.14
84	202.508	–29.531	14 298	300	1.96	9	0.31
85	202.454	–31.220	16 187	368	7.38	5	0.77
86	202.554	–28.224	10 039	308	1.40	7	0.21
87	202.726	–30.496	14 818	354	8.88	5	1.01
88	203.169	–33.123	14 553	606	34.15	33	1.33
89	202.909	–32.994	3575	113	0.06	6	0.07
90	203.416	–31.590	14 547	650	26.52	14	0.89
91	203.661	–35.160	14 895	297	1.19	7	0.19
92	203.635	–33.037	14 991	165	1.59	4	0.83
93	203.901	–33.895	3646	282	3.93	10	0.70
94	203.913	–31.869	14 356	145	1.19	8	0.80
95	203.874	–31.447	14 435	377	3.28	5	0.33
96	204.840	–35.617	15 398	503	17.06	23	0.96
97	205.178	–34.052	14 807	373	13.84	11	1.42
98	204.981	–29.747	23 296	618	13.21	4	0.49
99	205.537	–30.708	4587	140	1.04	9	0.75
100	205.591	–30.040	14 460	359	7.91	4	0.87
101	205.900	–29.906	23 380	219	3.98	4	1.18
102	206.459	–29.950	4450	73	0.24	8	0.65
103	206.472	–32.168	14 946	183	0.17	4	0.07
104	206.917	–32.880	11 996	589	31.28	55	1.29
105	206.645	–31.632	11 400	407	2.31	8	0.19
106	207.251	–30.563	4539	503	12.01	37	0.67
107	206.926	–32.660	10 424	163	1.80	7	0.96

Table 1. continued.

SSGC number	RA (2000)	Dec (2000)	$\langle V_r \rangle$ [km s^{-1}]	σ_r [km s^{-1}]	Mass [$\times 10^{13}$ $M_\odot$]	#mem.	R_{vir} [Mpc]
108	207.162	–28.938	14 773	123	0.31	9	0.29
109	207.691	–48.476	3022	263	3.14	5	0.65
110	207.389	–32.243	11 265	545	22.52	4	1.08
111	207.484	–30.207	22 294	496	27.91	8	1.62
112	207.955	–30.635	4438	368	6.76	10	0.71
113	207.590	–32.853	11 043	528	21.00	5	1.07
114	208.152	–28.642	4895	312	4.58	12	0.67
115	208.189	–32.865	11 204	210	2.45	5	0.79
116	208.404	–27.876	15 069	413	20.64	14	1.73
117	208.362	–30.340	22 259	271	8.33	8	1.61
118	208.643	–26.578	5703	232	4.71	5	1.25
119	210.625	–34.035	4220	419	17.65	39	1.43
120	209.597	–32.562	4402	161	1.47	6	0.80
121	210.572	–33.149	11 012	334	9.34	5	1.19
122	211.985	–27.024	6773	386	7.15	13	0.68

Table 2. Groups or clusters of galaxies previously identified close to SSGC groups.

SSGC number	System name	Type of system	Mean V_r [km s^{-1}]	$\Delta\theta$ [arc. min.]
SSGC 3	LGG 301	GGroup	...	10.6
SSGC 5	USGC S187	GGroup	3337	5.3
	ABELL S0714	GClstr	3258	6.0
SSGC 7	ABELL 3528	GClstr	15829	14.6
SSGC 8	ABELL 3528N	GClstr	15889	3.3
	AM 1252-285	GGroup	...	8.4
SSGC 12	ABELL 3530	GClstr	16099	12.4
SSGC 15	ABELL 3531	GClstr	22454	8.2
SSGC 16	ABELL 3532	GClstr	16609	2.6
SSGC 17	LGG 317	GGroup	...	4.0
SSGC 19	ABELL 3535	GClstr	19546	3.3
SSGC 20	ABELL S0717	GClstr	...	0.3
SSGC 25	AM 1258-320	GGroup	...	11.1
SSGC 28	NGC 4936 GROUP	GGroup	...	8.3
SSGC 29	ABELL 3537	GClstr	9593	13.4
SSGC 30	AM 1258-303	GGroup	...	3.9
SSGC 35	LGG 326	GGroup	...	19.2
SSGC 37	ABELL S0721	GClstr	14690	1.7
	VV 671	GGroup	...	1.9
SSGC 40	NGC 4965 GROUP	GGroup	...	9.6
SSGC 45	ABELL 3542	GClstr	15739	8.2
SSGC 47	ABELL 3545	GClstr	28270	15.8
SSGC 49	ABELL S0725	GClstr	...	3.1
SSGC 50	ABELL S0726	GClstr	17700	2.7
	SCL 128	GClstr	...	23.6
SSGC 51	SCL 129	GClstr	...	19.2
SSGC 53	AM 1315-365	GGroup	...	2.0
	ABELL 3553	GClstr	14600	8.5
SSGC 54	ABELL S0728	GClstr	...	18.6
SSGC 56	ABELL 3554	GClstr	14090	3.1
	AM 1316-330 NED02	GGroup	...	4.6
SSGC 61	ABELL 3555	GClstr	14630	10.5
SSGC 62	[BPR98] B0109	GGroup	...	11.7
SSGC 64	AM 1320-343	GGroup	...	2.5
SSGC 65	[BPR98] T075	GGroup	15075	4.9
	ABELL 3556	GClstr	14360	6.2
SSGC 66	AM 1320-330	GGroup	...	0.9
SSGC 67	CL 1322-30	GClstr	4222	6.6
	AM 1322-300	GGroup	...	7.8
SSGC 69	AM 1324-265	GClstr	...	9.3
SSGC 70	[BPR98] T260	GGroup	1472	14.6
SSGC 71	ABELL 1736 NED02	GClstr	13577	9.4
SSGC 73	[BPR98] T300	GGroup	14952	3.4
	ABELL 3558	GClstr	14390	5.0
SSGC 74	ABELL 1736 NED01	GClstr	10443	9.4
SSGC 78	[BPR98] B1014	GGroup	...	3.4
SSGC 81	SC1327-312	GCstr	14481	7.7
	[BPR98] T413	GGroup	15099	8.0
SSGC 82	[BPR98] T496	GGroup	14673	8.8
SSGC 83	[BPR98] T520	GGroup	13446	3.3
	SC1329-313	GGroup	14450	7.3
SSGC 84	HCG 065	GGroup	14240	1.6
	ABELL 3559	GClstr	13820	2.1

Table 2. continued.

SSGC number	System name	Type of system	Mean V_r [km s^{-1}]	$\Delta\theta$ [arc. min.]
SSGC 86	ABELL S0736	GClstr	...	15.0
SSGC 88	RX J1332.2-3303	GClstr	14090	7.7
	ABELL 3560	GClstr	14660	11.9
SSGC 90	[BPR98] T561	GGroup	14501	1.8
	ABELL 3562	GClstr	14690	5.3
	AM 1331-311 NED01	GGroup	...	7.3
SSGC 91	ABELL 3564	GClstr	15140	5.0
SSGC 93	ABELL 3565	GClstr	3687	14.0
SSGC 94	[BPR98] T599	GGroup	14426	2.5
SSGC 95	[BPR98] T598	GGroup	14991	13.9
SSGC 96	ABELL 3566	GClstr	15289	6.4
SSGC 98	AM 1337-292	GGroup	...	1.2
	SC 1340-294	GClstr	23229	1.5
SSGC 100	SC 1342-302	GClstr	14515	18.3
SSGC 104	ABELL 3571	GClstr	11722	2.6
SSGC 106	LGG 359	GGroup	...	9.5
SSGC 109	AM 1346-483	GGroup	...	19.5
SSGC 112	AM 1349-300	GGroup	...	23.2
SSGC 113	AM 1346-324	GGroup	...	16.0
SSGC 114	KLEMOLA 28	GGroup	...	11.5
SSGC 115	ABELL 3575	GClstr	11302	2.2
SSGC 116	ABELL 3577	GClstr	14810	9.8
SSGC 117	AM 1349-300	GGroup	...	9.3
SSGC 119	ABELL S0753	GClstr	4197	14.7
SSGC 122	ABELL 3581	GClstr	6895	6.4